View metadata, citation and similar papers at core.ac.uk

brought to you by CORE

provided by Copenhagen University Research Information System

UNIVERSITY OF COPENHAGEN

Hydroxyl radical-induced formation of highly oxidized organic compounds

Berndt, Torsten; Richters, Stefanie; Jokinen, Tuija; Hyttinen, Noora; Kurtén, Theo; Otkjær, Rasmus Vanglo; Kjærgaard, Henrik Grum; Stratmann, Frank; Herrmann, Hartmut; Sipilä, Mikko; Kulmala, Markku; Ehn, Mikael

Published in:
Nature Communications

DOI:
10.1038/ncomms13677

Publication date:
2016

Document version
Publisher's PDF, also known as Version of record

Document license:
CC BY

Citation for published version (APA):
Berndt, T., Richters, S., Jokinen, T., Hyttinen, N., Kurtén, T., Otkjær, R. V., ... Ehn, M. (2016). Hydroxyl radical-induced formation of highly oxidized organic compounds. *Nature Communications*, *7*, [13677]. https://doi.org/10.1038/ncomms13677

Download date: 08. Apr. 2020

nature COMMUNICATIONS

ARTICLE

Received 18 May 2016 | Accepted 25 Oct 2016 | Published 2 Dec 2016

DOI: 10.1038/ncomms13677 OPEN

Hydroxyl radical-induced formation of highly oxidized organic compounds

Torsten Berndt[1], Stefanie Richters[1], Tuija Jokinen[2], Noora Hyttinen[3], Theo Kurtén[3], Rasmus V. Otkjær[4], Henrik G. Kjaergaard[4], Frank Stratmann[1], Hartmut Herrmann[1], Mikko Sipilä[2], Markku Kulmala[2] & Mikael Ehn[2]

Explaining the formation of secondary organic aerosol is an intriguing question in atmospheric sciences because of its importance for Earth's radiation budget and the associated effects on health and ecosystems. A breakthrough was recently achieved in the understanding of secondary organic aerosol formation from ozone reactions of biogenic emissions by the rapid formation of highly oxidized multifunctional organic compounds via autoxidation. However, the important daytime hydroxyl radical reactions have been considered to be less important in this process. Here we report measurements on the reaction of hydroxyl radicals with α- and β-pinene applying improved mass spectrometric methods. Our laboratory results prove that the formation of highly oxidized products from hydroxyl radical reactions proceeds with considerably higher yields than previously reported. Field measurements support these findings. Our results allow for a better description of the diurnal behaviour of the highly oxidized product formation and subsequent secondary organic aerosol formation in the atmosphere.

[1] Leibniz-Institut für Troposphärenforschung (TROPOS), Permoserstraße 15, 04318 Leipzig, Germany. [2] Department of Physics, University of Helsinki, Helsinki 00014, Finland. [3] Department of Chemistry, University of Helsinki, Helsinki 00014, Finland. [4] Department of Chemistry, University of Copenhagen, Copenhagen 2100, Denmark. Correspondence and requests for materials should be addressed to T.B. (email: berndt@tropos.de).

Atmospheric aerosol particles play important roles in the climate[1,2], human health[3] and ecosystems. It is known that a dominant source of atmospheric aerosol particles is formation via oxidation of inorganic (for example, SO_2) and organic (for example, α- and β-pinene) precursor gases resulting in low vapour pressure reaction products[4]. However, both fundamental and quantitative knowledge, especially concerning the chemical pathways leading to the formation of aerosol particles from organic precursor gases, are still missing.

Ehn *et al.*[5] conclusively demonstrated the formation of highly oxidized multifunctional organic compounds (HOMs) from the ozonolysis of α-pinene and their importance to secondary organic aerosol (SOA) formation. HOMs can be partly classified as extremely low-volatility organic compounds[6] due to the expected low vapour pressures. The remaining fraction can be attributed to low- or semi-volatile organic compounds. An exact determination of the vapour pressure of HOMs is currently impossible preventing a more accurate classification. The HOM detection became feasible by the latest developments of online mass spectrometric techniques[7,8]. Other terpene ozonolysis studies[9–11], using the same detection technique, have confirmed the findings by Ehn *et al.*[5] and discovered that HOM formation with up to 12 O atoms in the molecules proceeds on a time scale of seconds at atmospheric reactant concentrations. More recently, first indications for the presence of HOMs from α-pinene ozonolysis were found in the particle phase[12].

The above observations suggest that especially the ozone reaction with terpenes is responsible for rapidly formed low-volatility SOA precursors. Up to now, laboratory studies[5,9,10], all using the nitrate ionization technique, indicate a minor importance of OH radical-driven HOM generation compared with ozonolysis. Estimated molar HOM yields of $<1\%$ (ref. 5) and $0.44^{+0.44}_{-0.22}\%$ (ref.10) from OH + α-pinene are reported using total signal measurements, that is, all appearing signals in a selected mass-to-charge range were taken into account without a specification of the respective reaction product. Atmospheric measurements, however, point to dominant particle formation and growth during daytime, indicating that there must be a large source of low-volatility organic species that is connected to the photochemistry[4]. The most important daytime oxidant in the atmosphere is the OH radical, whereas nighttime oxidation is dominated by ozone and the NO_3 radical[13].

The present work represents a specific study on HOM formation from the OH radical initiated oxidation of the most abundant monoterpenes emitted by vegetation, α- and β-pinene[14]. We measure the 'early' HOMs, that is, the highly oxidized RO_2 radicals, which represent the intermediates finally forming closed-shell HOMs in the atmosphere via different reaction pathways. These reaction pathways are, for example, bimolecular reactions with NO, NO_2, HO_2 and other RO_2 radicals or unimolecular reaction steps[13]. We find that these RO_2 radicals can be detected with good sensitivity[9,15], enhancing our ability to understand the HOM formation process in more detail. In our experiments designed to probe the highly oxidized RO_2 radical generation, consecutive bimolecular RO_2 radical reactions are unimportant because of low concentrations ($<10^7$ molecules cm^{-3}) and short reaction times in the range of 3.0–7.9 s. The HOM detection is carried out by means of chemical ionization–atmospheric pressure interface–time-of-flight (CI-APi-TOF) mass spectrometry (Airmodus, Tofwerk) with a detection limit of $\sim 10^4$ molecules cm^{-3}. A recent study indicated that nitrate ionization, the technique used in almost all HOM studies so far, may not be sensitive to all key HOM compounds[15]. Therefore, the experimental approach applied here comprises a set of four different reagent ions for product identification, that is, nitrate (NO_3^-), lactate ($CH_3CH(OH)COO^-$), pyruvate ($CH_3C(O)COO^-$) and acetate (CH_3COO^-), to probe the ion-specific detection efficiency. The investigations are conducted in a free-jet flow system at 295 ± 2 K and at atmospheric pressure[15]. Additional experiments with elevated HO_2 and RO_2 radical concentrations or NO additions are conducted, to probe qualitatively the closed-shell HOM formation starting from the highly oxidized RO_2 radicals. In conclusion, our results show the importance of the OH radical-induced formation of HOMs from monoterpenes. This finding allows a better description of the diurnal cycle of SOA formation by available HOMs formed either from the ozonolysis or via OH radical reactions.

Results

Reagent ion-dependent detection efficiency. In the experiments, a strong enhancement of the signals attributed to the OH radical-derived highly oxidized RO_2 radicals occurred after switching the reagent ion from nitrate to lactate, pyruvate or acetate. All detected RO_2 radicals were exclusively formed in the flow system as shown by experiments for characterizing the measurement system, (Supplementary Figs 1–3 and Supplementary Note 1). The spectra in Fig. 1a,b show the comparison of results from the ozonolysis of α-pinene (simultaneous O_3 and OH radical reaction) and from the pure OH + α-pinene reaction, respectively, using either nitrate or acetate for ionization. The occurrence of the strong signal at nominal 308 Th using acetate ionization (at nominal 311 Th for nitrate ionization) in both sets of experiments demonstrates that this product is formed from the OH radical attack on α-pinene without a contribution of any ozone reactions. In contrast to the OH radical-derived RO_2 radicals, the signal strength of RO_2 radicals from the simultaneous O_3 + α-pinene reaction remained almost unchanged switching from nitrate to acetate (Fig. 1a). A strong signal at nominal 308 Th appeared also in the case of the OH + β-pinene reaction using acetate ionization, in line with the findings from the α-pinene system (Supplementary Fig. 4).

The predominant signal of the OH radical-derived RO_2 radicals, observed by means of all four reagent ions, is consistent with the elemental formula $HO\text{-}C_{10}H_{16}O_6$. Experiments in the presence of heavy water allow the determination of acidic H atoms in the molecules (equal to the number of OH and OOH groups) by H/D exchange measuring the resulting signal shift in the mass spectrum[16], (Supplementary Fig. 5). The analysis revealed two acidic H atoms in $HO\text{-}C_{10}H_{16}O_6$, indicating a chemical composition of $\mathbf{H}O\text{-}C_{10}H_{15}(OO)(OO\mathbf{H})O_2$. Another composition of this species, including other functional groups such as ether or carboxylic groups, is implausible and would be contrary to the current knowledge of possible elementary steps in these reaction systems[5,9,11,15,16]. It should be noted that there is one acidic H atom less than expected, if all inserted O_2 into the molecule (beside the peroxy O_2 of the RO_2 radical) were present as OOH groups[9,15,16]. It can be speculated that the additional '(OO)' group stands for an endo-peroxide generated via ring closure of an unsaturated RO_2 radical. Such a process was predicted by theoretical calculations[17] and qualitatively confirmed by a product study from a chamber experiment[18]. The initial, unsaturated RO_2 radicals, species **4** and **7**, are formed from the OH radical reaction of α- and β-pinene with high yields (Fig. 2)[19,20]. Possible reaction pathways for the generation of the highly oxidized RO_2 radicals from the OH + α-pinene reaction have been proposed (Supplementary Figs 6–9). The pathways include an initial intramolecular H-shift[5,9,15,16,21], followed by O_2 addition leading to RO_2 radicals with five O atoms. Then a very rapid H-shift involving the OOH group[22] takes place followed by an endo-cyclization and a next O_2 addition to get the RO_2

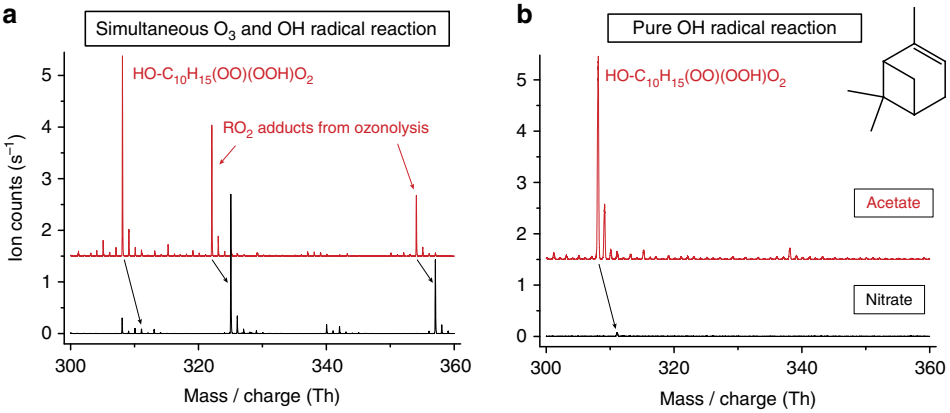

Figure 1 | Recorded mass spectra using acetate or nitrate for ionization. The detected RO_2 radicals from the oxidation of α-pinene appear as adducts with the reagent ions. Signals of nitrate adducts (black) are shifted by three mass units compared to the corresponding acetate adduct signals (red). The spectra obtained with acetate ionization are offset by 1.5 s^{-1} for more clarity. The reaction time in all experiments was 7.9 s. (**a**) Spectra obtained from α-pinene ozonolysis for identical conditions $[O_3] = 6.1 \times 10^{11}$ and $[\alpha\text{-pinene}] = 1.0 \times 10^{12}$ molecules cm^{-3}. Simultaneous O_3 and OH radical reaction takes place due to OH radical production from ozonolysis. (**b**) Spectra from the pure OH + α-pinene reaction using H_2O_2 photolysis for OH radical formation, $[H_2O_2] \sim 1 \times 10^{14}$ and $[\alpha\text{-pinene}] = 5.0 \times 10^{12}$ molecules cm^{-3}. The signal at nominal 309 Th (first isotope signal of the RO_2 radical) can be partly influenced by the corresponding hydroperoxide.

radicals **19**, **20** and **29** containing seven O atoms each. Based on quantum chemical calculations (Supplementary Tables 1–3 and Supplementary Note 2), the RO_2 radicals **19**, **20** and **29**, all with the chemical composition HO-$C_{10}H_{15}$(OO)(OOH)O_2, can be formed on a seconds time scale starting from the RO_2 radical **4** as illustrated in a simplified way in Fig. 2b. The calculations furthermore indicate that **19**, **20** and **29** are relatively stable with respect to further isomerization steps (H-shifts). For β-pinene, similar reaction steps are assumed. An additional minor signal appeared in the β-pinene spectra that was attributed to HO-$C_{10}H_{16}O_8$ (Supplementary Fig. 4). A composition **H**O-$C_{10}H_{14}$(OO)(OO**H**)$_2O_2$ can be assumed based on the H/D exchange results, which indicated three acidic H atoms in the molecule. It should be noted that the reaction sequence of RO_2 radical isomerization (H-shift or cyclization) followed by O_2 addition (Fig. 2) represents a reaction principle well known in low-temperature combustion chemistry[23].

Estimated molar HOM yields. The estimated RO_2 radical concentrations for both terpenes as a function of reacted α- and β-pinene gave a linear response for terpene conversions smaller than 4×10^8 molecules cm^{-3} (Fig. 3). This behaviour confirmed the absence of significant bimolecular RO_2 radical reactions for these experimental conditions. Different measurement series (I–III) revealed consistent and reproducible results. The stated radical concentrations, and consequently the yields, represent estimated lower end values for the different ionization schemes. Resulting molar yields of highly oxidized RO_2 radicals from OH + α-pinene are 2.4 ± 0.1% (acetate ionization) and 0.052 ± 0.006% (nitrate ionization). The corresponding values for OH + β-pinene are 0.90 ± 0.03% and 0.022 ± 0.001%, respectively. Given error limits comprise statistical errors only.

The estimated RO_2 radical yields deduced from nitrate ionization are about a factor of 40 smaller than those from acetate ionization pointing to more stable (OH-RO_2) · acetate adducts compared with the corresponding nitrate adducts. (Note: the factor of 40 is substance specific and not generally valid.) Theoretical calculations on the cluster stability of model RO_2 radicals with nitrate or acetate have been performed, which support the experimental findings of this study (Supplementary Figs 10 and 11, Supplementary Table 4 and Supplementary Note 3). When comparing the experiments using ionization by lactate and pyruvate with those applying acetate, the results differ by a factor smaller than two, indicating similar cluster stabilities for the organic reagent ions. In the case of the ozonolysis-derived RO_2 radicals, the four reagent ions yielded almost the same sensitivities within a factor of 1.6 (Supplementary Fig. 12).

Additional runs with NO and increased RO_2 concentrations. Furthermore, we tested the reactivity of the detected RO_2 radicals from the OH + α-pinene reaction towards NO and measured the resulting product formation for atmospherically relevant NO concentrations of (5.6–280) × 10^8 molecules cm^{-3} (Supplementary Fig. 13). An increasing signal, HO-$C_{10}H_{15}$(OO)(OOH)ONO_2, appeared with rising NO concentrations according to the organic nitrate formation via $RO_2 + NO \rightarrow RONO_2$ starting from HO-$C_{10}H_{15}$(OO)(OOH)O_2 (refs 9,15,24). Other signals were tentatively attributed to reaction products of the corresponding alkoxy radical, HO-$C_{10}H_{15}$(OO)(OOH)O, formed in a parallel way via $RO_2 + NO \rightarrow RO + NO_2$. The total amount of products indicates that the HO-$C_{10}H_{15}$(OO)(OOH)O_2 radical formation was not disturbed by the NO additions (Supplementary Fig. 13 and Supplementary Note 4). Thus, the RO_2 isomerization steps leading to HO-$C_{10}H_{15}$(OO)(OOH)O_2 must be faster than the corresponding RO_2 reactions with NO, which proceed with pseudo first-order rate coefficients of up to 0.28 s^{-1}. This estimate assumes a rate coefficient $k(NO + RO_2)$ of 1×10^{-11} cm^3 per molecule per second[24]. Consequently, the rate coefficients of the RO_2 isomerization steps forming the RO_2 radicals **19**, **20** and **29** must be larger than 0.28 s^{-1} in line with the results of theoretical calculations.

H_2O_2 photolysis experiments with increased reactant concentrations were conducted in the TROPOS flow tube[25]. For OH + α-pinene, the product formation from the reaction of the highly oxidized RO_2 radicals with HO_2 and other RO_2 radicals were studied (Supplementary Fig. 14a,b). The analysis of the mass spectra recorded for different RO_2/HO_2 ratios allowed a qualitative description of the respective reaction products. The reaction of HO-$C_{10}H_{15}$(OO)(OOH)O_2 with HO_2 yielded the corresponding hydroperoxide according to $RO_2 + HO_2 \rightarrow ROOH + O_2$. The main product from the reaction with other

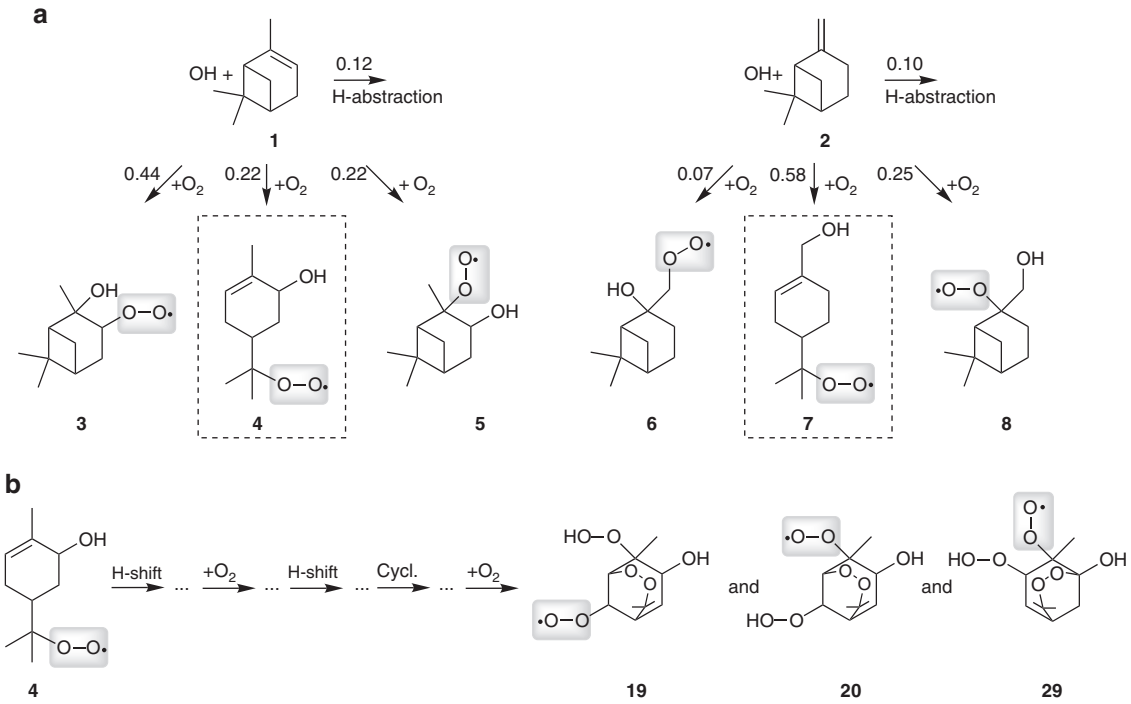

Figure 2 | Proposed reaction scheme for the formation of highly oxidized RO_2 radicals. (**a**) Formation of first RO_2 radicals from atmospheric OH radical reaction of α- and β-pinene. (**b**) Possible structures of highly oxidized RO_2 radicals **19**, **20** and **29**, HO-$C_{10}H_{15}$(OO)(OOH)O_2, formed from RO_2 radical **4** via a reaction sequence of isomerization steps (H-shift and cyclization) followed by O_2 addition. Branching ratios stated in **a** were taken from refs 19,20.

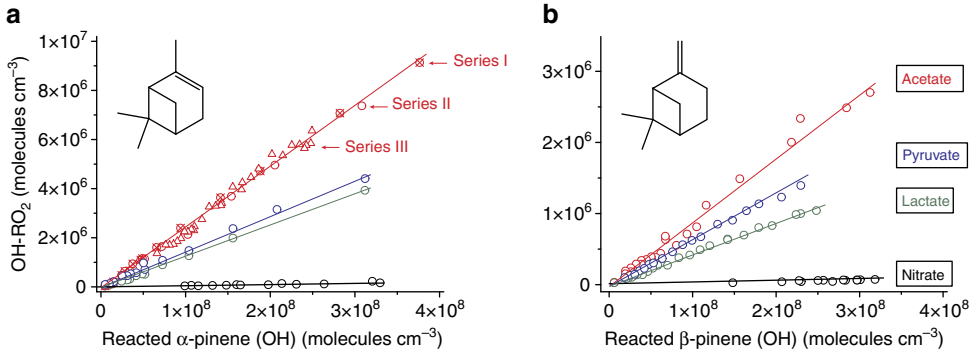

Figure 3 | Estimated RO_2 radical concentrations as a function of reacted α- and β-pinene. The given concentrations for the different reagent ions were obtained using a calibration factor from absolute sulphuric acid calibration that is in line with the calculated, lower end calibration factor of an ion-molecule reaction. Reagent ions (colour coding): nitrate (black), lactate (green), pyruvate (blue) and acetate (red). The reaction time in all experiments was 7.9 s. (**a**) α-Pinene reaction: series I and II from acetate ionization and the results from the other reagent ions were obtained from α-pinene ozonolysis with OH radical formation via O_3 + α-pinene. $[O_3] = 6.1 \times 10^{11}$ and [α-pinene] = (1.2–81) × 10^{10} molecules cm^{-3}. Series III (acetate ionization) shows findings from combined TME/α-pinene ozonolysis. O_3 + TME generates additional OH radicals. $[O_3] = 9.1 \times 10^{11}$, [TME] = (1.8–110) × 10^9, [α-pinene] = 1.0 × 10^{11} molecules cm^{-3}. (**b**) β-Pinene reaction: combined TME/β-pinene ozonolysis with preferred OH radical formation via the O_3 + TME reaction, $[O_3] = 9.1 \times 10^{11}$, [TME] = (1.8–95) × 10^9, [β-pinene] = 1.05 × 10^{11} molecules cm^{-3}.

RO_2 radicals was a species with −15 nominal mass units compared with the precursor RO_2 radical, probably HO-$C_{10}H_{15}$(OO)(OOH)OH. In the mass spectra also signals of C_{20} accretion products[5,9,11,15,16] appeared, which are consistent with the chemical formulas $C_{20}H_{34}O_8$, $C_{20}H_{34}O_{10}$ and $C_{20}H_{34}O_{12}$ (Supplementary Fig. 14b). Their formation can be mechanistically explained via $RO_2 + R'O_2 \rightarrow ROOR' + O_2$. RO_2 and $R'O_2$ represent the peroxy radicals from the OH + α-pinene reaction, which contain either three (species **3**, **4** or **5**), five (species **12**, **13** or **14**) or seven O atoms (species **19**, **20** or **29**).

We calculated the vapour pressure of three closed-shell C_{10} HOMs formed from the reaction of HO-$C_{10}H_{15}$(OO)(OOH)O_2 radicals with HO_2, NO or other RO_2 radicals using the increment method SIMPOL.1 (ref. 26) and the COSMO-RS approach[27]. All the estimated vapour pressures of the C_{10} products were below 10^{-9} atm at 295 K. Vapour pressures below 10^{-15} atm were determined for the C_{20} accretion products applying solely the SIMPOL.1 method[26] (Supplementary Table 5 and Supplementary Note 5). Thus, these highly oxidized products have a low volatility (and are water soluble) and can effectively condense on surfaces. Recently, SOA yields of 17–26% from low-NO α-pinene photooxidation experiments in the Caltech chamber were reported being independent of OH exposure[28]. This finding was not in line with SOA modelling results for this reaction system,

indicating the presence of other SOA formation routes, such as an autoxidation mechanism[5,9,21], not implemented in modelling schemes yet[28]. Our lower limit molar HOM yield from OH + α-pinene of 2.4% corresponds to a lower limit mass yield of 4.4% (average HOM mass: 250 g mol^{-1}). This mass yield can explain at least a fraction of the measured SOA yield from the Caltech experiments[28] and also from other SOA studies[29].

Comparison of laboratory and field measurements. Furthermore, field measurements from two different sites support the findings from the laboratory studies presented here. Figure 4a shows the time series of the most abundant, highly oxidized RO_2 radicals from terpene ozonolysis[9] (in black) and from the OH radical reaction (in red), as well as the corresponding organic nitrate (in green). The corresponding global radiation, serving as a proxy for the OH radical concentration, and the measured NO concentrations are depicted in Fig. 4b. The ozone concentration showed relatively small variation during the whole campaign (Supplementary Fig. 15). The measurements have been done at the boreal research station SMEAR II[30] in the spring 2011 using nitrate-CI-APi-TOF mass spectrometry. Considering an underestimation of the RO_2 concentrations from the OH radical reaction by a factor of 40 using nitrate ionization, as experimentally shown in this study, the corrected HO-$C_{10}H_{15}(OO)(OOH)O_2$ radical concentrations (dashed red line) reach peak concentrations of about 10^7 molecules cm^{-3} at daytime. This level clearly exceeds the ozonolysis-derived RO_2 radical concentrations. Further support for the atmospheric relevance of the OH radical initiated HOM formation comes from a 10-day measurement campaign at the TROPOS research station in Melpitz[31] in the summer 2013. Here, the diurnal pattern of the HO-$C_{10}H_{15}(OO)(OOH)O_2$ radical followed the diurnal trend of the global radiation, which was again used as a proxy for OH (Supplementary Fig. 16). This behaviour is consistent with the findings from the SMEAR II station.

Atmospheric lifetimes of RO_2 radicals regarding the reaction with other RO_2, HO_2 and NO are in the range of 1.7–170 min for the individual reactions assuming trace gas concentrations for non-urban conditions of 10^9 molecules cm^{-3} for RO_2 and HO_2 radicals, and NO each, $k(RO_2 + RO_2) \sim 1 \times 10^{-12}$–$10^{-13}$, $k(HO_2 + RO_2) \sim 1 \times 10^{-11}$ and $k(NO + RO_2) \sim 1 \times 10^{-11}$ cm^3 per molecule per second[24]. Taking all these bimolecular steps together, a RO_2 lifetime of a few minutes has to be taken into account. The nocturnal HO-$C_{10}H_{15}(OO)(OOH)O_2$ radical decline as given in Fig. 4a, however, indicates a RO_2 lifetime of a few hours. It could be speculated that (i) changing air masses with changing trace gas composition or (ii) boundary layer effects, or (iii) the non-zero nighttime OH radical reaction with terpenes influenced the nocturnal RO_2 concentration. In addition, instrumental uncertainties cannot be totally ruled out for the nighttime measurements close to the detection limit.

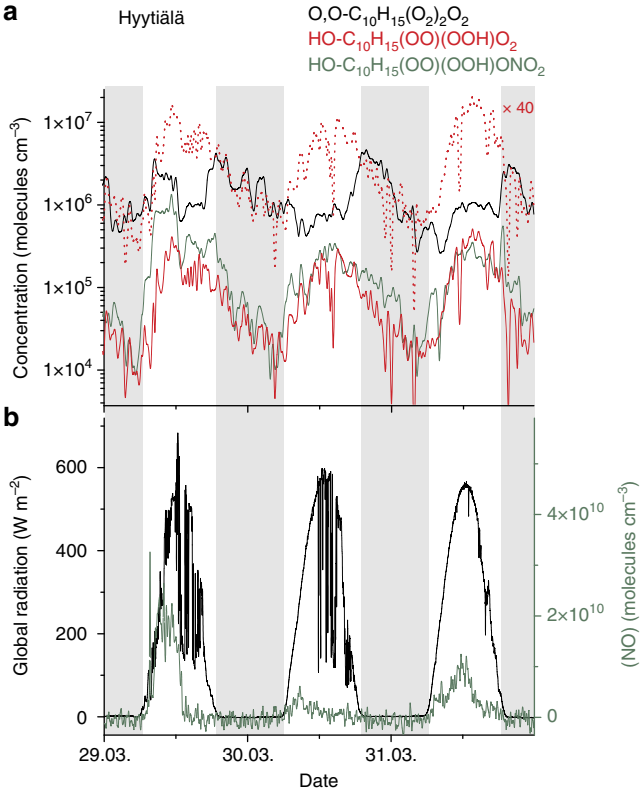

Figure 4 | Field measurements at the SMEAR II station. Hyytiälä, Finland, 29–31 March 2011. (**a**) Time series of the estimated concentrations of O,O-$C_{10}H_{15}(O_2)_2O_2$ radicals (in black) from ozonolysis of terpenes and HO-$C_{10}H_{15}(OO)(OOH)O_2$ radicals (in red) from the OH radical reaction as well as the corresponding organic nitrate (in olive). Full lines show the measurements by the nitrate-CI-APi-TOF mass spectrometer, the dashed red line stands for the corrected HO-$C_{10}H_{15}(OO)(OOH)O_2$ radical trace assuming an enhanced sensitivity by a factor of 40 based on the comparison of results using nitrate or acetate ionization in the laboratory experiments. (**b**) Global radiation is taken as a proxy for OH radicals. Enhanced NO concentration especially in morning hours of 29 March yielded enhanced organic nitrate concentrations.

Discussion

Our results clearly demonstrate the importance of the OH radical initiated oxidation of monoterpenes for a rapid formation of HOMs in the atmosphere. The findings of this work, together with the known process based on the ozonolysis of biogenic emissions[5,8,9], allow a more precise description of the diurnal behaviour of HOM generation and subsequent SOA formation, from the different oxidants. The participation of OH radical reactions for HOM formation is in agreement with the fact that both photochemistry and HOMs seem to be important in atmospheric particle formation processes[5].

Furthermore, several studies indicate a strong quantitative disagreement between experimentally observed SOA formation from field campaigns and model simulations based on laboratory data[32–35]. For instance, Russell *et al.*[34] observed for photooxidation conditions, most likely to be dominated by the OH radical reactions of α- and β-pinene, up to two orders of magnitude higher SOA generation compared with model predictions. The results of our study are able to overcome this discrepancy, at least qualitatively. However, also for urban areas with prevalent anthropogenic emissions, much larger amounts of SOA are reported than predicted by models[35]. Volkamer *et al.*[35] determined that a significant fraction of the excess SOA was formed from first-generation oxidation products of the anthropogenic emissions. It could be speculated that similar reaction pathways of HOM formation, as shown in our study for OH radical reaction with α- and β-pinene, take place in the course of the degradation of anthropogenic emissions, such as aromatics. However, a simple transfer of our results to other reaction systems is impossible due to the substance-specific reactivity of the RO_2 isomerization steps. Especially in this field, much more experimental and theoretical works are needed, to clarify the formation pathways of SOA precursors generated from anthropogenic emissions.

Methods

Free-jet flow system. The experiments have been performed in a free-jet flow system at a pressure of 1 bar purified air (or O_2/N_2 mixtures) and a temperature of 295 ± 2 K (refs15,36). The reaction time was in the range of 3.0–7.9 s. This set-up allows the investigation of oxidation reaction for atmospheric conditions in absence of wall effects.

The free-jet flow system consists of an outer tube (length: 200 cm, inner diameter: 15 cm) and a moveable inner tube (outer diameter: 9.5 mm) equipped with a nozzle. Ozone or H_2O_2 premixed with the carrier gas (5 l min^{-1} STP, standard temperature and pressure) is injected through the inner tube into the main gas stream (95 l min^{-1} STP), which contains the second reactant (α- or β-pinene). Large differences of the gas velocities at the nozzle outflow (nozzle: 15.9 m s^{-1}; main flow: 0.13 m s^{-1}) and the nozzle geometry ensure rapid reactant mixing downstream the nozzle. Diffusion processes at 1 bar air are too slow to transport a significant fraction of the reaction products out of the centre flow towards the walls within the time range of this experiment (3.0–7.9 s).

Ozone was produced by passing 1–2 l min^{-1} (STP) air through an ozone generator (UVP OG-2) and blended with carrier gas to a total flow of 5 l min^{-1} (STP) taken as the feed for the inner tube. In the case of H_2O_2 photolysis experiments, a flow of 0.03–1.0 l min^{-1} air (STP) over a H_2O_2 sample (saturator maintained at 273 K) supplied the oxidant feed. Photolysis was carried out downstream the mixing point of the gas streams by means of 8 low-pressure ultraviolet lamps emitting in the range 300–320 nm (Cosmedico Licht GmbH, ARIMED B6).

Additional photolysis experiments were conducted in the TROPOS flow tube[25] at a temperature of 293 ± 0.5 K using synthetic air as the carrier gas. The first flow-tube section (56 cm) contains the inlet system for the reactant gases (air mixed with α-pinene and H_2O_2 taken from a saturator as described before). A second section (344 cm) surrounded by 8 ultraviolet lamps (Hg-lamps made of quartz-glass PN235 with a cutoff wavelength of 210 nm) represents the photolysis zone. The sampling outlets are attached at the non-irradiated end section (~20 cm). The total gas flow was set at 20 l min^{-1} (STP) resulting in a reaction time of 48 s.

Ozone was followed by means of a gas monitor (Thermo Environmental Instruments 49C). The concentrations of α- and β-pinene and tetramethylethylene (TME) were detected with the help of a proton transfer reaction mass spectrometer (Ionicon, PTR-MS 500)[37].

All gas flows were set by means of calibrated gas flow controllers (MKS 1259/1179). The chemicals and gases had the following purity: α-pinene (99.5%, Fluka), β-pinene (99.0%, Fluka), TME (2,3-dimethyl-2-butene, 99%, Aldrich), acetic acid (99.5%, Aldrich), lactic acid (~90%, Merck), pyruvic acid (98%, Fluka), NO (98.5%, Aldrich), N_2 (99.9997%, AirProducts) and O_2 (99.9992%, AirProducts). Air was taken from a commercial PSA (Pressure Swing Adsorption) unit with further purification by activated charcoal, 4 Å molecular sieve and subsequently by GateKeeper CE-2500KH084R, Entegris.

CI-APi-TOF mass spectrometer and HOM quantification. Detection of highly oxidized products was carried out using a CI-APi-TOF mass spectrometer (Airmodus, Tofwerk) sampling the centre flow through a sampling inlet (length: 28 cm, inner diameter: 1.6 cm) with a rate of 10 l min^{-1} (STP). Another sampling inlet with a similar geometry allows dilution of the sample flow by a factor of 7 using arbitrary dilution gases. Applied reagent ions were nitrate (NO_3^-), acetate (CH_3COO^-), lactate ($CH_3CH(OH)COO^-$) and pyruvate ($CH_3C(O)COO^-$). A flow of 0.5–5 ml min^{-1} air over a concentrated acid sample (HX: nitric acid, acetic acid, lactic acid or pyruvic acid) was added to a 35 l min^{-1} (STP) flow of purified air producing the HX containing sheath air that forms the charger ions, X^-, $(HX)X^-$ and $(HX)_2X^-$, after ionization with a ^{241}Am source. Highly oxidized organic products are able to form stable $(HOM)X^-$ clusters as already shown for nitrate adducts ($X^- \equiv NO_3^-$)[5,9,11,15,16,38] and acetate adducts ($X^- \equiv CH_3COO^-$)[15]. Proton transfer from the HOM to the charger ion, as described for measurements by acetate ionization[39,40], was found to be negligible in this reaction system. HOM concentrations were determined according to equation (1). The values given in the brackets are the measured ion signals.

$$[\mathrm{HOM}] = f_{\mathrm{HOM}} \frac{[(\mathrm{HOM})\mathrm{X}^-]}{[\mathrm{X}^-] + [(\mathrm{HX})\mathrm{X}^-] + [(\mathrm{HX})_2\mathrm{X}^-]} \quad (1)$$

Absolute signal calibration is impossible due to the lack of HOM reference substances. The lower end value of the calibration factor f_{HOM} can be calculated considering the $(HOM)X^-$ adduct formation in the CI-inlet via reaction (2), $f_{\mathrm{HOM,calc}} = 1/(k \times t \times f_{\mathrm{inlet}})$[5,41], where k is the rate coefficient of the ion-molecule reaction, t the reaction time and the term f_{inlet} considers the sample (HOM) loss in the sampling tube.

$$\mathrm{HOM} + (\mathrm{HX})_n\mathrm{X}^- \rightarrow (\mathrm{HOM})\mathrm{X}^- + (\mathrm{HX})_n,\ n=0,1,2 \quad (2)$$

The rate coefficient $k = k_2$ is set to $k_2 = (2\text{–}3) \times 10^{-9}$ cm^3 per molecule per second, typical for a series of ion-molecule reactions close to the collision limit[42,43]. Taking into account a 12% diffusion loss of the sample (HOM) in the short sampling tube (diffusion controlled wall loss for an assumed diffusion coefficient $D = 0.08$ cm^2 s^{-1}), $f_{\mathrm{inlet}} = 0.88$ and a reaction time of the ion-molecule reaction $t = 0.2\text{–}0.3$ s, $f_{\mathrm{HOM,calc}} = (1.3\text{–}2.8) \times 10^9$ molecules cm^{-3} follows. The only reliable absolute calibration at the moment in our system is that used for sulphuric acid detection via $H_2SO_4 + (HNO_3)_nNO_3^-$, $n = 0, 1, 2, 3$ (refs 44,45) with a calibration factor $f_{\mathrm{H2SO4,exp}} = 1.85 \times 10^9$ molecules cm^{-3} (ref. 46). This value is in good agreement with the range of $f_{\mathrm{HOM,calc}}$, the lower end value of f_{HOM}. By practical reasons (using a definite value of the calibration factor and not a range), f_{HOM} in equation (1) was set equal to $f_{\mathrm{H2SO4,exp}}$. The total uncertainty of the lower end determination of HOM concentration according to equation (1) is estimated with a factor of 2 including changing ion transmission in the considered mass range[7] as well.

Identical voltage settings in the mass spectrometer were applied for the four ionization techniques (reagent ion: nitrate, acetate, lactate and pyruvate) as optimized for low fragmentation measurements in the nitrate ionization mode.

Determination of reacted α- and β-pinene. The reaction conditions chosen in the free-jet experiments (low reactant concentrations, reactant conversion: << 1%) did not allow measuring the amount of converted α- and β-pinene. Concentrations of reacted α- and β-pinene from ozonolysis reactions were calculated based on a simple reaction scheme.

$$\mathrm{O_3} + \alpha\text{-pinene} \rightarrow 0.85\,\mathrm{OH} + \ldots \quad (3)$$

$$\mathrm{OH} + \alpha\text{-pinene} \rightarrow \mathrm{products} \quad (4)$$

$$\mathrm{O_3} + \beta\text{-pinene} \rightarrow 0.35\,\mathrm{OH} + \ldots \quad (5)$$

$$\mathrm{OH} + \beta\text{-pinene} \rightarrow \mathrm{products} \quad (6)$$

$$\mathrm{O_3} + \mathrm{TME} \rightarrow 1.0\,\mathrm{OH} + \ldots \quad (7)$$

$$\mathrm{OH} + \mathrm{TME} \rightarrow \mathrm{products} \quad (8)$$

OH radical yields from ozonolysis and the rate coefficients at 295 K were taken from the literature[13]: (unit: cm^3 per molecule per second) $k_3 = 1.1 \times 10^{-16}$, $k_4 = 5.3 \times 10^{-11}$, $k_5 = 2.24 \times 10^{-17}$, $k_6 = 7.8 \times 10^{-11}$, $k_7 = 1.0 \times 10^{-15}$ and $k_8 = 1.1 \times 10^{-10}$. Other OH radical reactions than those with the fed alkenes are negligible.

Converted α- and β-pinene via the OH radical reaction or via ozonolysis was calculated by numerical integration of the resulting ODE system according to pathways (3)–(8).

Initial reactant concentration of the ozonolysis experiments were:

(i) pure ozonolysis of α-pinene: $[O_3] = 6.1 \times 10^{11}$, [α-pinene] = (1.2–250) × 10^{10} molecules cm^{-3}.
(ii) simultaneous ozonolysis of TME/α-pinene: $[O_3] = 9.1 \times 10^{11}$, [TME] = (1.8–110) × 10^9, [α-pinene] = 1.0 × 10^{11} molecules cm^{-3}.
(iii) simultaneous ozonolysis of TME/β-pinene: $[O_3] = 9.1 \times 10^{11}$, [TME] = (1.8–100) × 10^9, [β-pinene] = 1.05 × 10^{11} molecules cm^{-3}

The calculation of converted α- and β-pinene from the H_2O_2 photolysis experiments was impossible due to the lack of a precise measurement technique for H_2O_2. Thus, only qualitative information can be obtained from the photolysis runs.

Unwanted bimolecular RO_2 reactions in the free-jet experiment. The basic idea of the ozonolysis-based OH radical experiments performed in the free-jet flow system was to conduct the reaction under conditions of negligible bimolecular RO_2 reactions. We are not able to measure total RO_2 and HO_2 radical concentrations in our experiment. As a conservative estimate, it is assumed that the total RO_2 as well as the HO_2 radical concentration did not exceed the amount of reacted terpene of $< 8 \times 10^8$ molecules cm^{-3}. Rate coefficient of the $RO_2 + RO_2$ and the $HO_2 + RO_2$ reactions are assumed to be in the range of $k(RO_2 + RO_2) \sim 1 \times 10^{-12}$–$10^{-13}$ cm^3 per molecule per second and $k(HO_2 + RO_2) \sim 1 \times 10^{-11}$ cm^3 per molecule per second[24]. From this, first-order rate coefficients for the stated upper reactant concentration limit are derived as $k^{1st}(RO_2) < 8 \times 10^{-4}$ s^{-1} and $k^{1st}(HO_2) < 8 \times 10^{-3}$ s^{-1}. The corresponding lifetimes are > 21 min and > 2.1 min, respectively. In the case of NO, a background concentration smaller than 1×10^8 molecules cm^{-3} can be deduced from the experiments with NO additions. In those, even for an NO addition of 5.6×10^8 molecules cm^{-3}, clear product signals from $NO + RO_2$ were visible (Supplementary Fig. 13), which were absent without NO additions. An assumed rate coefficient $k(NO + RO_2)$ of 1×10^{-11} cm^3 per molecule per second[24] yields a first-order rate coefficients of $< 1 \times 10^{-3}$ s^{-1} for NO concentrations smaller than 1×10^8 molecules cm^{-3} corresponding to a RO_2-lifetime with respect to the NO reaction of more than 16 min.

Consequently, any bimolecular reactions of RO_2 radicals with other RO_2 radicals, HO_2 or NO cannot be competitive with the RO_2 isomerization steps proceeding at a time scale of seconds or less.

Data availability. The data that support the findings of this study are available from the corresponding author upon reasonable request.

References

1. Von Schneidemesser, E. *et al.* Chemistry and the linkages between air quality and climate change. *Chem. Rev.* **115,** 3856–3897 (2015).
2. IPCC. *Climate Change 2013: The Physical Science Basis. Contribution of Working Group I to the Fifth Assessment Report of the Intergovernmental Panel on Climate Change* (Cambridge Univ. Press, 2013).
3. Davidson, C. I., Phalen, R. F. & Solomon, P. A. Airborne particulate matter and human health: a review. *Aerosol Sci. Technol.* **39,** 737–749 (2005).
4. Kulmala, M. *et al.* Direct observations of atmospheric aerosol nucleation. *Science* **339,** 943–946 (2013).
5. Ehn, M. *et al.* A large source of low-volatility secondary organic aerosol. *Nature* **506,** 476–479 (2014).
6. Donahue, N. M., Kroll, J. H., Pandis, S. N. & Robinson, A. L. A two-dimensional volatility basis set–Part 2: Diagnostics of organic-aerosol evolution. *Atmos. Chem. Phys.* **12,** 615–634 (2012).
7. Junninen, H. *et al.* A high-resolution mass spectrometer to measure atmospheric ion composition. *Atmos. Meas. Tech.* **3,** 1039–1053 (2010).
8. Jokinen, T. *et al.* Atmospheric sulphuric acid and neutral cluster measurements using CI-APi-TOF. *Atmos. Chem. Phys.* **12,** 4117–4125 (2012).
9. Jokinen, T. *et al.* Rapid autoxidation forms highly oxidized RO_2 radicals in the atmosphere. *Angew. Chem. Int. Ed.* **53,** 14596–14600 (2014).
10. Jokinen, T. *et al.* Production of extremely low volatile organic compounds from biogenic emissions: Measured yields and atmospheric implications. *Proc. Natl. Acad. Sci. USA* **112,** 7123–7128 (2015).
11. Mentel, T. F. *et al.* Formation of highly oxidized multifunctional compounds: autoxidation of peroxy radicals formed in the ozonolysis of alkenes–deduced from structure–product relationships. *Atmos. Chem. Phys.* **15,** 6745–6765 (2015).
12. Mutzel, A. *et al.* Highly oxidized multifunctional organic compounds observed in tropospheric particles: a field and laboratory study. *Environ. Sci. Technol.* **49,** 7754–7761 (2015).
13. Calvert, J. G. *et al. The Mechanism of Atmospheric Oxidation of the Alkenes* (Oxford Univ. Press, 2000).
14. Sindelarova, K. *et al.* Global data set of biogenic VOC emissions calculated by the MEGAN model over the last 30 years. *Atmos. Chem. Phys.* **14,** 9317–9341 (2014).
15. Berndt, T. *et al.* Gas-phase ozonolysis of cycloalkenes: formation of highly oxidized RO_2 radicals and their reactions with NO, NO_2, SO_2, and other RO_2 radicals. *J. Phys. Chem. A* **119,** 10336–10348 (2015).
16. Rissanen, M. P. *et al.* The formation of highly oxidized multifunctional products in the ozonolysis of cyclohexene. *J. Am. Chem. Soc.* **136,** 15596–15606 (2014).
17. Vereecken, L., Müller, J.-F. & Peeters, J. Low-volatility poly-oxygenates in the OH-initiated atmospheric oxidation of α-pinene: impact of non-traditional peroxyl radical chemistry. *Phys. Chem. Chem. Phys.* **9,** 5241–5248 (2007).
18. Eddingsaas, N. C., Loza, C. L., Yee, L. D., Seinfeld, J. H. & Wennberg, P. O. α-Pinene photooxidation under controlled chemical conditions–Part 1: gas-phase composition in low- and high-NO_x environments. *Atmos. Chem. Phys.* **12,** 6489–6504 (2012).
19. Peeters, J., Vereecken, L. & Fantechi, G. The detailed mechanism of the OH-initiated atmospheric oxidation of α-pinene: a theoretical study. *Phys. Chem. Chem. Phys.* **3,** 5489–5504 (2001).
20. Vereecken, L. & Peeters, J. A theoretical study of the OH-initiated gas-phase oxidation mechanism of β-pinene ($C_{10}H_{16}$): first generation products. *Phys. Chem. Chem. Phys.* **14,** 3802–3815 (2012).
21. Crounse, J. D., Nielsen, L. B., Jørgensen, S., Kjaergaard, H. G. & Wennberg, P. O. Autoxidation of organic compounds in the atmosphere. *J. Phys. Chem. Lett.* **4,** 3513–3520 (2013).
22. Jørgensen, S. *et al.* Rapid hydrogen shift scrambling in hydroperoxy-substituted organic peroxy radicals. *J. Phys. Chem. A* **120,** 266–275 (2016).
23. Gardiner, Jr W. C. (ed.) *Gas-Phase Combustion Chemistry* 2nd edn (Springer Verlag, 2000).
24. Lightfoot, P. D., Cox, R. A., Crowley, M., Hayman, G. D. & Zabel, F. Organic peroxy radicals: Kinetics, spectroscopy and tropospheric chemistry. *Atmos. Environ. A* **26,** 1805–1961 (1992).
25. Berndt, T., Böge, O., Stratmann, F., Heintzenberg, J. & Kulmala, M. Rapid formation of sulfuric acid particles at near-atmospheric conditions. *Science* **307,** 698–700 (2005).
26. Pankow, J. F. & Asher, W. E. SIMPOL.1: a simple group contribution method for predicting vapor pressures and enthalpies of vaporization of multifunctional organic compounds. *Atmos. Phys. Chem.* **8,** 2773–2796 (2008).
27. Eckert, F. & Klamt, A. Fast solvent screening via quantum chemistry: COSMO-RS approach. *AIChE Journal* **48,** 369–385 (2002).
28. McVay, R. C. *et al.* SOA formation from the photooxidation of α-pinene: systematic exploration of the simulation of chamber data. *Atmos. Chem. Phys.* **16,** 2785–2802 (2016).
29. Mutzel, A. *et al.* Monoterpene SOA – contribution of first-generation oxidation products to formation and chemical composition. *Atmos. Environ.* **130,** 136–144 (2015).
30. Hari, P. & Kulmala, M. Station for measuring ecosystem – atmosphere relations (SMEAR II). *Boreal Env. Res.* **10,** 315–322 (2005).
31. Spindler, G. *et al.* Long-term size-segregated particle (PM10, PM2.5, PM1) characterization study at Melpitz – influence of air mass inflow, weather conditions and season. *J. Atmos. Chem.* **70,** 165–195 (2013).
32. Heald, C. H. *et al.* A large organic aerosol source in the free troposphere missing from current models. *Geophys. Res. Lett.* **32,** L18809 (2005).
33. Hallquist, M. *et al.* The formation, properties and impact of secondary organic aerosol: current and emerging issues. *Atmos. Chem. Phys.* **9,** 5155–5236 (2009).
34. Russell, L. M. *et al.* Nanoparticle growth following photochemical α- and β-pinene oxidation at Appledore Island during international Consortium for research on transport and transformation/chemistry of halogens at the Isles of Shoals 2004. *J. Geophys. Res.* **112,** D10S21 (2007).
35. Volkamer, R. *et al.* Secondary organic aerosol formation from anthropogenic air pollution: rapid and higher than expected. *Geophys. Res. Lett.* **33,** L17811 (2006).
36. Berndt, T. *et al.* Kinetics of the unimolecular reaction of CH_2OO and the bimolecular reactions with the water monomer, acetaldehyde and acetone at atmospheric conditions. *Phys. Chem. Chem. Phys.* **17,** 19862–19873 (2015).
37. Lindinger, W., Hansel, A. & Jordan, W. Proton-transfer-reaction mass spectrometry (PTR–MS): on-line monitoring of volatile organic compounds at pptv levels. *Chem. Soc. Rev.* **27,** 347–375 (1998).
38. Hyttinen, H. *et al.* Modeling the detection of highly oxidized cyclohexene ozonolysis products using nitrate-based chemical ionization. *J. Phys. Chem. A* **119,** 6339–6345 (2015).
39. Veres, P. *et al.* Development of negative-ion proton-transfer chemical-ionization mass spectrometry (NI-PT-CIMS) for the measurement of gas-phase organic acids in the atmosphere. *Int. J. Mass Spectrom.* **274,** 48–55 (2008).
40. Bertram, T. *et al.* A field-deployable, chemical ionization time-of-flight mass spectrometer. *Atmos. Meas. Tech.* **4,** 1471–1479 (2011).
41. Berresheim, H., Elste, T., Plass-Dülmer, C., Eisele, F. L. & Tanner, D. J. Chemical ionization mass spectrometer for long-term measurements of atmospheric OH and H_2SO_4. *Int. J. Mass Spectrom.* **202,** 91–109 (2000).
42. Viggiano, A. A. *et al.* Rate constants for the reactions of $XO_3^-(H_2O)_n$ (X = C, HC, and N) and $NO_3^-(HNO_3)_n$ with H_2SO_4: implications for atmospheric detection of H_2SO_4. *J. Phys. Chem. A* **101,** 8275–8278 (1997).
43. Mackay, G. I. & Bohme, D. K. Proton-transfer reactions in nitromethane at 297 K. *Intern. J. Mass Spectrom. Ion Phys.* **26,** 327–343 (1978).
44. Eisele, F. L. & Tanner, D. J. Measurement of the gas phase concentration of H_2SO_4 and methane sulfonic acid and estimates of H_2SO_4 production and loss in the atmosphere. *J. Geophys. Res.* **98,** 9001–9010 (1993).
45. Mauldin, III R. L. *et al.* OH measurements during the first aerosol characterization experiment (ACE-1): observations and model comparisons. *J. Geophys. Res.* **103,** 16713–16729 (1998).
46. Berndt, T. *et al.* H_2SO_4 formation from the gas-phase reaction of stabilized Criegee intermediates with SO_2: Influence of water vapour content and temperature. *Atmos. Environ.* **89,** 603–612 (2014).

Acknowledgements

We thank K. Pielok, A. Rohmer and the station teams from Hyytiälä and Melpitz for technical assistance and the tofTools team for providing the data analysis tools. This work was partly funded by the ACTRIS IA (2011–2015) project, the PEGASOS (FP7-ENV-2010-265148) project and by the European Research Council (COALA, grant 638703).

Author contributions

T.B. and S.R. did the laboratory experiments and analysed the data. T.B. and F.S. designed the free-jet flow experiment. T.J. and M.S. did the measurements and data analyses of SMEAR II experiments. T.B., M.E., H.H. and M.K. contributed mainly to the data interpretation. N.H., T.K., R.V.O. and H.G.K. performed the theoretical calculations. T.B. wrote the manuscript and all authors contributed to the final manuscript development.

Additional information

Supplementary Information accompanies this paper at http://www.nature.com/naturecommunications

Competing financial interests: The authors declare no competing financial interests.

Reprints and permission information is available online at http://npg.nature.com/reprintsandpermissions/

How to cite this article: Berndt, T. *et al.* Hydroxyl radical-induced formation of highly oxidized organic compounds. *Nat. Commun.* **7,** 13677 doi: 10.1038/ncomms13677 (2016).

Publisher's note: Springer Nature remains neutral with regard to jurisdictional claims in published maps and institutional affiliations.

This work is licensed under a Creative Commons Attribution 4.0 International License. The images or other third party material in this article are included in the article's Creative Commons license, unless indicated otherwise in the credit line; if the material is not included under the Creative Commons license, users will need to obtain permission from the license holder to reproduce the material. To view a copy of this license, visit http://creativecommons.org/licenses/by/4.0/

© The Author(s) 2016